Anal. Chem. **2001,** *73,* 1560−1566

Mammalian Cell Cultures on Micropatterned Surfaces of Weak-Acid, Polyelectrolyte Hyperbranched Thin Films on Gold

Mary Lee Amirpour,[†] Pradyut Ghosh,[‡] William M. Lackowski,[‡] Richard M. Crooks,*[,‡] and Michael V. Pishko*[,†]

Department of Chemical Engineering, Texas A&M University, College Station, Texas 77843-3122, and Department of Chemistry, Texas A&M University, P.O. Box 30012, College Station, TX 77842-3012.

A four-step soft lithographic process based on microcontact printing of organic monolayers, hyperbranched polymer grafting, and subsequent polymer functionalization results in polymer/*n*-alkanethiol patterns that direct the growth and migration of mammalian cells. The functional units on these surfaces are three-dimensional cell "corrals" that have walls 52 ± 2 nm in height and lateral dimensions on the order of 60 μm. The corrals have hydrophobic, methyl-terminated *n*-alkanethiol bottoms, which promote cell adhesion, and walls consisting of hydrophilic poly(acrylic acid)/poly(ethylene glycol) layered nanocomposites that inhibit cell growth. Cell viability studies indicate that cells remain viable on the patterned surfaces for up to 21 days, and fluorescence microscopy studies of stained cells demonstrate that cell growth and spreading does not occur outside of the corral boundaries. This simple, chemically flexible micropatterning method provides spatial control over growth of IC-21 murine peritoneal macrophages, human umbilical vein endothelial cells, and murine hepatocytes.

We recently reported a method for preparing micrometer-scale patterns of hyperbranched poly(acrylic acid) (PAA) thin films[1] and subsequently showed that one additional synthetic step, involving addition of a conformal coating of methoxy-terminated poly(ethylene glycol) amine ($MeOPEG_{5000}NH_2$, PEG) atop the PAA, inhibits bioadhesion.[2] Additionally, we found that these PAA/PEG composite films co-patterned with a methyl-terminated *n*-alkylthiol monolayer[3] direct the growth of macrophage cells.[2] Here we expand upon these findings by demonstrating the generality of this approach. Specifically, we report that three different mammalian cell types (macrophage, endothelial, and hepatocytes) can be patterned using this strategy and that such cells remain viable and spread to fill the "corrals" defined by the PAA/PEG boundaries.

The spatial control of mammalian cell adhesion and growth is a critical issue in many areas of biotechnology and especially biosensing using whole cells.[4,5] The goal of whole cell biosensing is to use molecular recognition and biochemical pathways inherent in cell function to sense complex analytes, for example, chemical/biological warfare agents and pathogens in food. Thus, micropatterned surfaces of the type described here could potentially be used as a template to direct the growth of multiple cell types into addressable arrays.

Because cellular adhesion and spreading is regulated by protein adsorption, patterning of proteins responsible for cellular adhesion leads to spatially directed cellular adhesion.[6−8] Surface adsorption of patterned adhesion proteins can be accomplished by exposure of substrates with varying protein affinity to protein-containing media. Several studies have demonstrated cellular adhesion by this route,[9−13] and it has been found that surface properties such as hydrophobicity and hydrophilicity,[14,15] surface charge,[16−18] and surface roughness[16,19] affect protein adsorption.

* Authors to whom correspondence should be addressed. R.M.C.: (voice) 979-845-5629; (fax) 979-845-1399; (e-mail) crooks@tamu.edu. M.V.P.: (voice) 979-847-9395; (fax) 979-845-6446; (e-mail) pishko@tamu.edu.

[†] Department of Chemical Engineering.

[‡] Department of Chemistry.

(1) Lackowski, W. M.; Ghosh, P.; Crooks, R. M. *J. Am. Chem. Soc.* **1999**, *121*, 1419−1420.

(2) Ghosh, P.; Amirpour, M. L.; Lackowski, W. M.; Pishko, M. V.; Crooks, R. M. *Angew. Chem., Int. Ed. Engl.* **1999**, *38*, 1592−1595.

(3) Nuzzo, R. G.; Allara, D. L. *J. Am. Chem. Soc.* **1983**, *105*, 4481−4483.

(4) Pancrazio, J. J.; Bey, P. P.; Cuttino, D. S.; Kusel, J. K.; Borkholder, D. A.; Shaffer, K. M.; Kovacs, G. T. A.; Stenger, D. A. *Sens. Actuators, B* **1998**, *53*, 179−185.

(5) O'Connor, S. M.; Andreadis, J. D.; Shaffer, K. M.; Ma, W.; Pancrazio, J. J.; Stenger, D. A. *Biosens. Bioelectron.* **2000**, *14*, 871−881.

(6) Dewez, J. L.; Lhoest, J. B.; Detrait, E.; Berger, V.; Dupontgillain, C. C.; Vincent, L. M.; Schneider, Y. J.; Bertrand, P.; Rouxhet, P. G. *Biomaterials* **1998**, *19*, 1441−1445.

(7) Thomas, C. H.; McFarland, C. D.; Jenkins, M. L.; Rezania, A.; Steele, J. G.; Healy, K. E. *J. Biomed. Mater. Res.* **1997**, *37*, 81−93.

(8) Saneinejad, S.; Shoichet, M. S. *J. Biomed. Mater. Res.* **1998**, *42*, 13−19.

(9) Prime, K. L.; Whitesides, G. M. *Science* **1991**, *252*, 1164−1167.

(10) Prime, K. L.; Whitesides, G. M. *J. Am. Chem. Soc.* **1993**, *115*, 10714−10721.

(11) Stenger, D. A.; Georger, J. H.; Dulcey, C. S.; Hickman, J. J.; Rudolph, A. S.; Nielsen, T. B.; McCort, S. M.; Calvert, J. M. *J. Am. Chem. Soc.* **1992**, *114*, 8435−8442.

(12) Böltau, M.; Walheim, S.; Mlynek, J.; Krausch, G.; Steiner, U. *Nature* **1998**, *391*, 877−879.

(13) Tidwall, C. D.; Ertel, S. I.; Ratner, B. D.; Tarasevich, B.; Atre, S.; Allara, D. L. *Langmuir* **1997**, *13*, 3404−3413.

(14) McGurk, S. L.; Green, R. J.; Sanders, G. H. W.; Davies, M. C.; Roberts, C. J.; Tendler, S. J. B.; Williams, P. M. *Langmuir* **1999**, *15*, 5136−5140.

(15) Detrait, E.; Lhoest, J.-B.; Bertrand, P.; Van den Bosch de Aguilar, P. *J. Biomed. Mater. Res.* **1999**, *45*, 404−413.

(16) Hallab, N. J.; Bundy, K. J.; O'Conner, K.; Clark, R.; Moses, R. L. *J. Long-Term Effects Med. Implants* **1995**, *5*, 209−231.

(17) Luck, M.; Paulke, B.-R.; Schroder, W.; Blunk, T.; Muller, R. H. *J. Biomed. Mater. Res.* **1998**, *39*, 478−485.

10.1021/ac000907f CCC: $20.00 © 2001 American Chemical Society
Published on Web 02/27/2001

For example, PEG is one material that has been shown to be quite efficient in resisting adsorption of proteins responsible for cellular adhesion.[20−24] Methods used to pattern substrates for cell growth have included photolithography[25−31] and microcontact printing (μCP).[5,32−44] μCP is a soft lithographic method that employs an elastomeric stamp to print chemical ink on surfaces with micrometer and even submicrometer resolution.[45−50] Our studies[1,2] rely upon μCP of *n*-alkylthiol monolayers, followed by subsequent polymer grafting steps, to yield three-dimensional composite polymeric patterns that direct cell adhesion and spreading. The polymeric patterns reported here require more synthetic overhead than purely monolayer patterns, which have also been shown to direct cell growth, but because of their three-dimensional structure they are more chemically versatile and less prone to structural defects and delamination.[51−54]

Scheme 1

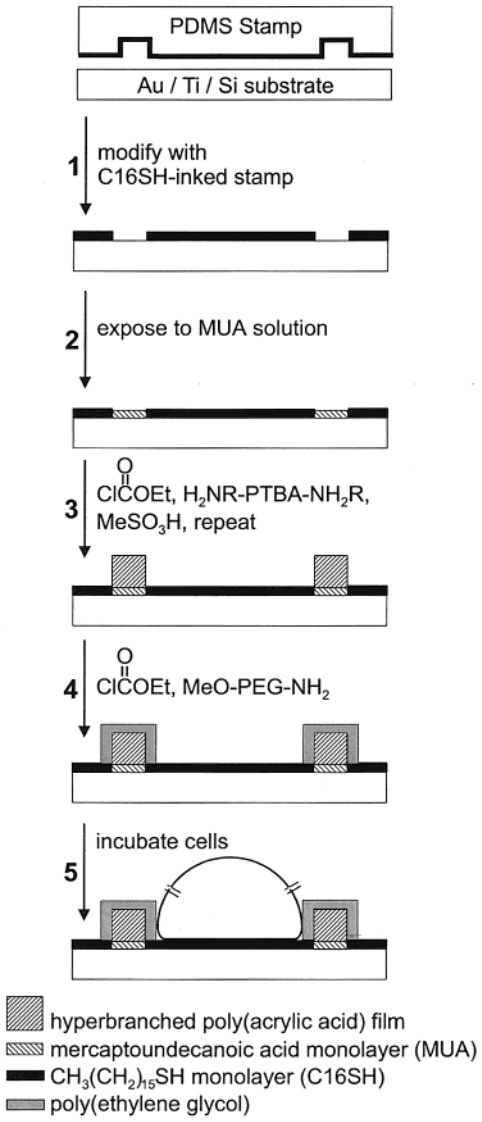

Four basic steps are required to prepare three-dimensional biopatterns (Scheme 1): μCP-based lithography, monolayer patterning, hyperbranched polymer grafting, and subsequent polymer functionalization. The key aspects of this approach are that hyperbranched PAA polymer growth only occurs on regions of the substrate that were originally modified with monolayers having reactive terminal acid groups and that grafting errors, which could lead to subsequent bioadhesion errors, are eliminated by the

(18) Qiu, Q.; Sayer, M.; Kawaja, M.; Shen, X.; Davies, J. E. *J. Biomed. Mater. Res.* **1998**, *42*, 117−127.
(19) Dufrene, Y. F.; Marchal, T. G.; Rouxhet, P. G. *Langmuir* **1999**, *15*, 2871−2878.
(20) Zhang, M. Q.; Desai, T.; Ferrari, M. *Biomaterials* **1998**, *19*, 953−960.
(21) Pertsin, A. J.; Grunze, M.; Garbuzova, I. A. *J. Phys. Chem. B* **1998**, *102*, 4918−4926.
(22) Harder, P.; Grunze, M.; Dahint, R.; Whitesides, G. M.; Laibinis, P. E. *J. Phys. Chem. B* **1998**, *102*, 426−436.
(23) Freij-Larsson, C.; Nylander, T.; Jannasch, P.; Wesslen, B. *Biomaterials* **1996**, *17*, 2199−2207.
(24) Sheth, S. R.; Leckband, D. *Proc. Natl. Acad. Sci. U.S.A.* **1997**, *94*, 8399−8904.
(25) Blawas, A. S.; Oliver, T. F.; Pirrung, M. C.; Reichert, W. M. *Langmuir* **1998**, *14*, 4243−4250.
(26) Matsuzawa, M.; Krauthamer, V.; Potember, R. S. *BioSystems* **1995**, *35*, 199−202.
(27) Matsuda, T.; Sugawara, T. *J. Biomed. Mater. Res.* **1995**, *29*, 749−756.
(28) Ravenscroft, M. S.; Bateman, K. E.; Shaffer, K. M.; Schessler, H. M.; Jung, D. R.; Schneider, T. W.; Montgomery, C. B.; Custer, T. L.; Schaffner, A. E.; Liu, Q. Y.; Li, Y. X.; Barker, J. L.; Hickman, J. J. *J. Am. Chem. Soc.* **1998**, *120*, 12169−12177.
(29) Tai, H.-C.; Buettner, H. M. *Biotechnol. Prog.* **1998**, *14*, 364−370.
(30) Vaidya, R.; Tender, L. M.; Bradley, G.; O'Brien, M. J.-I.; Cone, M.; López, G. P. *Biotechnol. Prog.* **1998**, *14*, 371−377.
(31) Bergman, A. A.; Buijs, J.; Herbig, J.; Mathes, D. T.; Demarest, J. J.; Wilson, C. D.; Reimann, C. T.; Baragiola, R. A.; Hull, R.; Oscarssson, S. O. *Langmuir* **1998**, *14*, 6785−6788.
(32) López, G. P.; Albers, M. W.; Schreiber, S. L.; Carroll, R.; Peralta, E.; Whitesides, G. M. *J. Am. Chem. Soc.* **1993**, *115*, 5877−5878.
(33) Singhvi, R.; Kumar, A.; López, G. P.; Stephanopoulos, G. N.; Wang, D. I. C.; Whitesides, G. M.; Ingber, D. E. *Science* **1994**, *264*, 696−698.
(34) Chen, C. S.; Mrksich, M.; Huang, S.; Whitesides, G. M.; Ingber, D. E. *Science* **1997**, *276*, 1425−1428.
(35) Chen, C. S.; Mrksich, M.; Huang, S.; Whitesides, G. M.; Ingber, D. E. *Biotechnol. Prog.* **1998**, *14*, 356−363.
(36) Britland, S.; Clark, P.; Conolly, P.; Moores, G. *Exp. Cell Res.* **1992**, *198*, 124−129.
(37) Branch, D. W.; Corey, J. M.; Weyhenmeyer, J. A.; Brewer, G. J.; Wheeler, B. C. *Med. Biol. Eng. Comput.* **1998**, *36*, 135−141.
(38) Mrksich, M. *Cell. Mol. Life Sci.* **1998**, *54*, 653−662.
(39) Mrksich, M.; Dike, L. E.; Tien, J.; Ingber, D. E.; Whitesides, G. M. *Exp. Cell Res.* **1997**, *235*, 305−313.
(40) Mrksich, M.; Whitesides, G. M. *Annu. Rev. Biophys. Biomol. Struct.* **1996**, *25*, 55−78.
(41) James, C. D.; Davis, R. C.; Kam, L.; Craighead, H. G.; Isaacson, M.; Turner, J. N.; Shain, W. *Langmuir* **1998**, *14*, 741−744.
(42) Bernard, A.; Delamarche, E.; Schmid, H.; Michel, B.; Bosshard, H. R.; Biebuyck, H. *Langmuir* **1998**, *14*, 2225−2229.
(43) Wheeler, B. C.; Corey, J. M.; Brewer, G. J.; Branch, D. W. *J. Biomech. Eng.* **1999**, *121*, 73−78.
(44) Jenkins, A. T. A.; Bushby, R. J.; Boden, N.; Evans, S. D.; Knowles, P. F.; Liu, Q.; Miles, R. E.; Ogier, S. D. *Langmuir* **1998**, *14*, 4675−4678.
(45) Xia, Y. N.; Whitesides, G. M. *Angew. Chem., Int. Ed. Engl.* **1998**, *37*, 551−575.
(46) Jackman, R. J.; Brittain, S. T.; Adams, A.; Prentiss, M. G.; Whitesides, G. M. *Science* **1998**, *280*, 2089−2091.
(47) Huck, W. T. S.; Tien, J.; Whitesides, G. M. *J. Am. Chem. Soc.* **1998**, *120*, 8267−8268.
(48) Clark, S. L.; Montague, M. F.; Hammond, P. T. *Macromolecules* **1997**, *30*, 7237−7244.
(49) Jeon, N. L.; Lin, W.; Erhardt, M. K.; Girolami, G. S.; Nuzzo, R. G. *Langmuir* **1997**, *13*, 3833−3838.
(50) St. John, P. M.; Davis, R.; Cady, N.; Czajka, J.; Batt, C. A.; Craighead, H. G. *Anal. Chem.* **1998**, *70*, 1108−1111.
(51) Bruening, M. L.; Zhou, Y.; Aguilar, G.; Agee, R.; Bergbreiter, D. E.; Crooks, R. M. *Langmuir* **1997**, *13*, 770−778.
(52) Zhao, M.; Zhou, Y.; Bruening, M. L.; Bergbreiter, D. E.; Crooks, R. M. *Langmuir* **1997**, *13*, 1388−1391.
(53) Zhou, Y.; Bruening, M. L.; Liu, Y.; Crooks, R. M.; Bergbreiter, D. E. *Langmuir* **1996**, *12*, 5519−5521.
(54) Zhou, Y.; Bruening, M. L.; Bergbreiter, D. E.; Crooks, R. M.; Wells, M. *J. Am. Chem. Soc.* **1996**, *118*, 3773−3774.

hyperbranched polymer growth. Ellipsometry, FT-IR-external reflection spectroscopy (FT-IR-ERS), tapping mode atomic force microscopy (TM-AFM), X-ray photoelectron spectroscopy (XPS), and optical microscopy all indicate that it is possible to pattern cellular corrals" that have "fences" up to 52 ± 2 nm thick and critical lateral dimensions on the order of 2 μm. As we show here, these corrals contain IC-21 murine peritoneal macrophages, human umbilical vein endothelial cells, and murine hepatocytes without evidence for breaching of the corral fences or other placement errors even over areas as large as 1 cm^2. Moreover, a fluorescent assay indicates that cells within corrals remain viable for at least 3 weeks.

EXPERIMENTAL SECTION

Materials and Chemicals. 1,1′-Carbonyldiimidazole, 4,4′-azobis(4-cyanovaleric acid) (75+%), ethylenediamine (99%), 11-mercaptoundecanoic acid (MUA), hexadecanethiol (C16SH), *N*-methylmorpholine, ethyl chloroformate, methanesulfonic acid, *tert*-butyl acrylate, and all anhydrous solvents were purchased from Aldrich Chemical Co. (Milwaukee, WI) and used without further purification except for the *tert*-butyl acrylate, which was distilled before use to remove polymerization inhibitors. Methoxy poly(ethylene glycol) amine molecular weight 5000 (Shearwater Polymers, Huntsville, AL) was used as received. Murine hepatocytes SV40 transformed BALB/c H2.35 (CRL-1995), human umbilical cord endothelial cells HUV-EC-C (CRL-1730), and SV40 transformed murine IC-21 peritoneal macrophages (TIB-186) were obtained from American Type Culture Collection (Manassas, VA). Dulbecco's modified Eagle's medium, dexamethasone, fetal bovine serum (FBS), F12K medium, sodium bicarbonate, heparin, antibiotic/antimycotic solution, RPMI 1640 medium, glucose, HEPES, sodium pyruvate, sodium chloride, potassium phosphate monobasic, trypsin, and ethylenediaminetetraacetate (EDTA) were obtained from Sigma Chemical Co. (St. Louis, MO). LIVE/DEAD Viability/Cytotoxicity Kit (L-7013) and BODIPY FL phallacidin (B-607) were purchased from Molecular Probes (Eugene, OR). Endothelial cell growth supplement (ECGS) was obtained from Collaborative Biomedical Products (Bedford, MA). Hexamethyldisilazane was purchased from Ted Pella, Inc. (Redding, CA). Phosphate-buffered saline solutions (PBS) were prepared using sodium chloride, potassium phosphate monobasic, and sodium phosphate dibasic heptahydrate.

Microfabrication of Patterned Surfaces. The general approach for preparing the patterned surfaces used in this work, which we have described previously,[1,2] is given in Scheme 1. Prior to seeding with cells, substrates were sterilized by exposure to 365-nm ultraviolet light in a bath of sterile PBS overnight or by steam autoclaving at 120 °C for 15 min. Neither sterilization technique resulted in measurable film loss or modification, as verified by bright-field optical microscopy, FT-IR-ERS, and ellipsometry.

Characterization. FT-IR-ERS measurements were made using a Bio-Rad FTS-6000 spectrometer equipped with a Harrick Scientific Seagull reflection accessory and liquid N_2-cooled narrow-band MCT detector. All spectra were the sum of 256 or fewer individual scans with *p*-polarized light at an 84° angle of incidence with respect to the Au substrate.

Ellipsometric thickness measurements were performed on films in air using a Gaertner model L2W26D ellipsometer (Chicago, IL) with a 70° angle of incidence at 633-nm wavelength. Refractive indexes (n_f) and film thicknesses were calculated by assuming a standard homogeneous film model using Gaertner software. To calculate the thickness of dry PAA or PAA/PEG films, refractive indexes of 1.54 and 1.46, respectively, were used. These refractive index values were determined using ellipsometry on thicker films where they can be quantitatively determined.

Contact angles were measured in air with a FTA 200 goniometer using deionized water. The contact angle values reported are the average of four measurements obtained at different locations on the films. The estimated error is ±3°.

TM-AFM images of patterned 3-PAA/PEG films with and without adherent cells were obtained in air using a Digital Instruments Nanoscope III (Santa Barbara, CA) fitted with a 200-μm *j* scanner. Tapping-mode cantilevers (NanoSensors, Wetzlar-Blankenfeld, Germany) had resonance frequencies between 260 and 280 kHz, force constants of 20−100 N/m, and tip apex radii of ∼10 nm. Images were acquired at 512 × 512 pixels at 0.1−0.5 Hz using a near-minimal contacting force. To follow the topography of patterned cell surfaces, the STM gain settings were set at values larger than usual (integral 1.5−2.5; proportional 15−25.) The resulting images were flattened and plane-fit using Digital Instruments software.

Cell Culture Conditions. All cell lines were incubated at 37 °C in 5% CO_2, 95% air. Murine macrophages were cultured in RPMI 1640 medium with 2 mM L-glutamine containing 1.5 g/L sodium bicarbonate, 4.5 g/L glucose, 10 mM HEPES, 1.0 mM sodium pyruvate 90%, and fetal bovine serum 10%. Cells were grown to confluence in 75-cm^2 polystyrene tissue culture flasks and subcultured biweekly. Murine hepatocytes were grown in Dulbecco's modified Eagle's medium containing 1.0 g/L glucose, 200 nM dexamethasone, and 4% FBS. HUV-EC-C were grown in F12K medium containing 2 mM L-glutamine, 1.5 g/L sodium bicarbonate, 100 μg/mL heparin, 30−50 μg/mL ECGS, and 10% fetal bovine serum. Confluent HUV-EC-C cells and hepatocytes were subcultured by trypsinization with 0.25% (w/v) trypsin and 0.13% (w/v) EDTA. Confluent macrophages were subcultured using a cell scraper in PBS. Cells were plated on sterilized substrates at a density of 1.0×10^5 cells/mL in all experiments except for cells plated on 3-PAA patterned films, which were plated at 1.0×10^4 cells/mL. After 24 h, the cells adherent to the substrate were either fixed and imaged by bright-field optical microscopy (Axiophot, Zeiss) or assayed for viability or cytoskeletal structure.

Cell Viability Assays. A LIVE/DEAD Reduced Biohazard Viability/Cytotoxicity fluorescence assay was used to investigate cell viability on patterned surfaces. This assay uses two fluorophores: SYTO 10, which is green and membrane-permeable, and DEAD RED, which is red and only stains cells with compromised membranes. After 24 h of incubation, media covering the cells adherent on the patterned surfaces was removed and the surface was washed with HBSS. The fluorophore mixture was placed on the sample, incubated in darkness for 15 min at room temperature, and then removed. The cells were washed with HBSS and fixed using 4% glutaraldehyde for 60 min. The fixative was then removed and the samples were imaged using fluorescence microscopy.

Cell Cytoskeletal Assays. BODIPY FL phallacidin was used to investigate the F-actin cytoskeleton of cells adherent on the patterned surfaces. After 24 h of incubation, medium, covering

Scheme 2

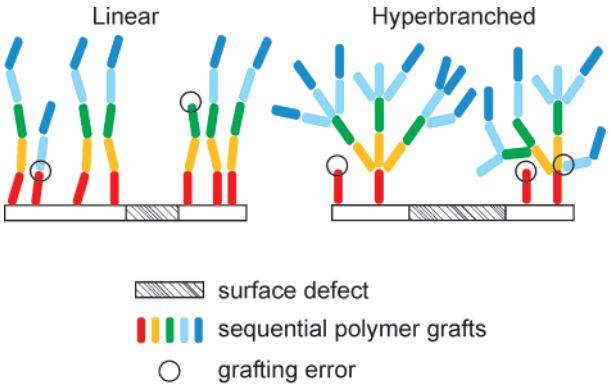

cells adherent on the patterned surfaces was removed and the surface washed with PBS (pH 7.4). Samples were then fixed in a 3.7% formaldehyde solution in PBS for 10 min after which they were washed with PBS. Samples were then covered with acetone at room temperature for 5 min after which they were washed with PBS. The BODIPY FL fluorescent staining solution was applied for 20 min. Samples were washed with PBS, allowed to air-dry, and then imaged using fluorescence microscopy.

RESULTS AND DISCUSSION

Characterization of Microfabricated Patterns. Our approach for preparing patterns that spatially direct the growth of cells is shown in Scheme 1. First, C16SH from a PDMS stamp is transferred to a Au substrate, which results in formation of a patterned monolayer film. Using the C16SH monolayer as an adhesion mask, the remainder of the Au surface is modified with a MUA self-assembled monolayer (SAM). Extended exposure of the patterned substrate to MUA (>∼1 min) leads to exchange of C16SH for MUA and ultimately to PAA grafting errors within the corrals. Activation of the carboxylic acid terminal groups of the MUA-patterned portions of the two-component monolayer is achieved via formation of a mixed anhydride, and subsequent reaction with α,ω-diamino-terminated poly(*tert*-butyl acrylate) (H_2NR-PTBA-RNH_2, PTBA) yields the grafted polymer layer. PTBA is subsequently hydrolyzed with $MeSO_3H$ to yield the first layer of PAA. Two more cycles of activation, grafting, and hydrolysis yield a hyperbranched 3-PAA film (the numeral reflects the number of activation, grafting, and hydrolysis cycles). Importantly, these films are self-healing in the sense that defects originally present in the MUA monolayer are eventually covered by the hyperbranched film (Scheme 2). For the same reason, coverage defects are not introduced even if the number of grafting defects (e.g., the percentage of unreacted acid groups) is very high (Scheme 2). Importantly, hyperbranched PAA films contain a high density of acid groups, which can subsequently be functionalized with a conformal layer of $MeOPEG_{5000}NH_2$ via simple amidation chemistry. This conformal layer inhibits adhesion of proteins and cells on the PAA films.

FT-IR-ERS, XPS, ellipsometry, and contact angle measurements confirm PAA grafting and subsequent functionalization with PEG only on MUA-modified regions of the Au surface. These studies also indicate that covalent attachment of PEG occurs primarily at the surface of the 3-PAA film.[2]

We have previously confirmed transfer of the 25-nm-thick 3-PAA film onto the Au substrate by TM-AFM.[1] Here we image

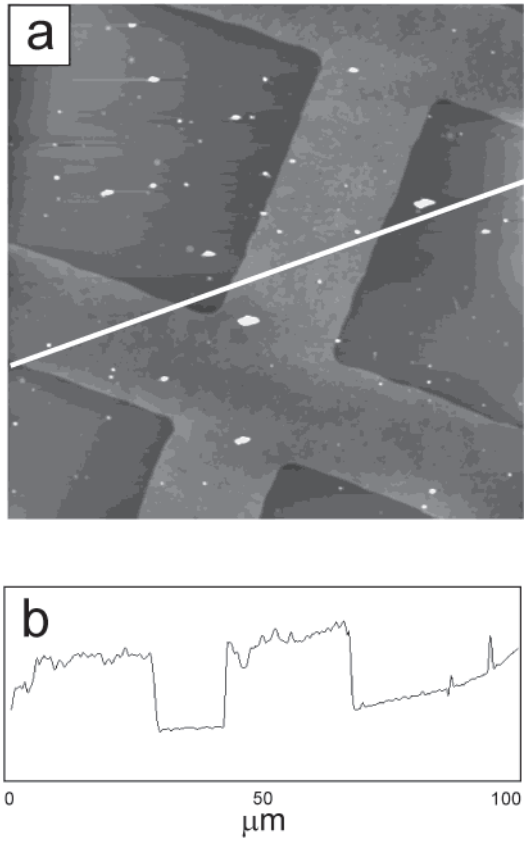

Figure 1. (a) 100 μm × 100 μm TM-AFM image of a patterned 3-PAA/PEG hyperbranched polymer film; (b) line scan spanning the white line in (a).

3-PAA/PEG patterns, providing insight into the spatial resolution and perfection of these patterns. Figure 1 shows TM-AFM images of corrals having 3-PAA/PEG walls and C16SH bottoms. The height difference between the top of the dry 3-PAA/PEG film and the top of the 1.8-nm-thick C16SH monolayer is 52 ± 2 nm, which is consistent with the ellipsometrically determined thickness of identically prepared unpatterned films. The corrals are 63 μm square and the walls are 20 μm wide. The total area of a single corral is ∼4 × 10^{-5} cm^2. The interface between 3-PAA/PEG and C16SH is on the order of 500 nm.

Protein Adsorption and Cell Adsorption and Spreading on Patterned Substrates. Cellular adhesion onto a surface is normally preceded by adsorption of proteins.[55−57] Accordingly, it is reasonable to assume that if protein adsorption can be controlled, then cell growth and spreading will also be controlled. As mentioned earlier, PEG has previously been shown to resist adsorption by both cells and proteins.[24,58] Therefore, an overlayer of PEG grafted onto the PAA-covered fraction of a patterned substrate should inhibit protein adsorption. Figure 2 is an optical micrograph of a 3-PAA/PEG and C16SH pattern that confirms this supposition. The surface was exposed to a bovine serum

(55) van Wachem, P. B.; Vreriks, C. M.; Beugeling, T.; Feijen, J.; Bantjes, A.; Detmers, J. P.; van Aken, W. G. *J. Biomed. Mater. Res.* **1987**, *21*, 701−718.
(56) Kaehler, J.; Zilla, P.; Fasol, R.; Deutsch, M.; Kadletz, M. *J. Vasc. Surg.* **1989**, *9*, 535−541.
(57) Ostuni, E.; Yan, L.; Whitesides, G. M. *Coll. Surf. B.* **1999**, *15*, 3−30.
(58) Harris, J. M., Zalipsky, S., Eds. *Poly(ethylene glycol). Chemistry and Biological Applications*; ACS Symposium Series 489; American Chemical Society: Washington, DC, 1997.

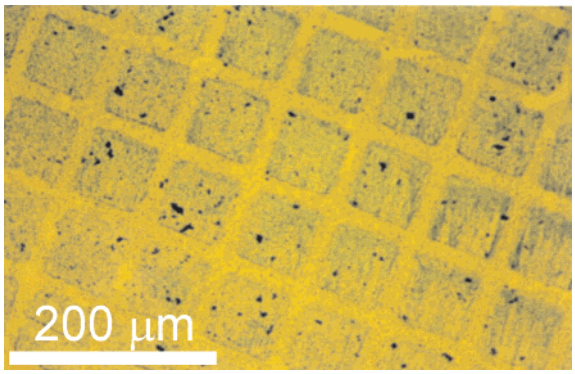

Figure 2. Optical micrograph of BSA adsorbed onto a pattern consisting of C16SH corrals and 3-PAA/PEG walls. To enhance visualization, the protein has been stained with Coomassie. Protein adsorption occurs preferentially on the C16SH portion of the pattern (squares).

albumin (BSA) solution for 4 h. After incubation in media, the pattern was rinsed and the adherent protein stained with Coomassie stain. A much higher density of the stained protein is present in the C16SH regions (corral interiors) of the surface. In the absence of protein adsorbed on the patterned substrate, Coomassie dye does not stain the pattern. Protein patterns similar to that shown in Figure 2 have previously been prepared on monolayer films,[10,32,59] and monolayers of proteins themselves have recently been patterned directly by μCP.[42] While these studies do not definitively show that protein adsorption does not occur on a 3-PAA/PEG surface, they do show that protein adsorption is significantly less than that on C16SH monolayers.

We[2] and others[9,10,57,60] previously reported that macrophage cells adhere and spread on patterned and unpatterned methyl-terminated SAMs. We have also shown that cells seed onto hyperbranched 3-PAA films, whereas composite 3-PAA/PEG-modified surfaces inhibit adsorption and growth.[2] There is precedence in the literature for these findings.[13,24,32] Interestingly, the cell density on homogeneous films of 3-PAA is about half that found on C16SH monolayers (700 vs 1400 cells/mm^2, respectively). This may be in part due to the relative surface roughness of 3-PAA and C16SH thin films[61] but most likely results principally from the much higher surface energy of PAA compared to the methyl-terminated SAM.[62,63]

Figure 3 shows patterned Au surfaces onto which macrophage cells have been seeded. The pattern in part a of Figure 3 consists of C16SH corrals surrounded by 3-PAA walls onto which PEG has *not* been grafted. In this case, the cells generally seed within the corrals, but they quickly spread into nearby corrals. In contrast, when a conformal layer of PEG is grafted onto the corral walls, the cells are fully contained (parts b and c of Figure 3). Indeed, we find that ~99% of cells are unable to escape from their corrals. If a corral is occupied by a low density of cells, as in part b, spreading by cell elongation (similar to that observed on tissue culture polystyrene) is typically observed.[64] Part c is a high-resolution optical micrograph of a single corral. Remarkably, even though this corral contains about nine macrophages, they are unable to grow onto or over the walls. The important point is that regardless of the cell growth mode or cell density, cell processes stop when they encounter the 3-PAA/PEG barrier. As described in the Experimental Section, serum-containing medium was used for all cell types investigated. Serum-free media and selective adsorption of extracellular matrix proteins prior to cell seeding were not required to permit patterning as is required for some cell patterning techniques that have been reported.[11,36]

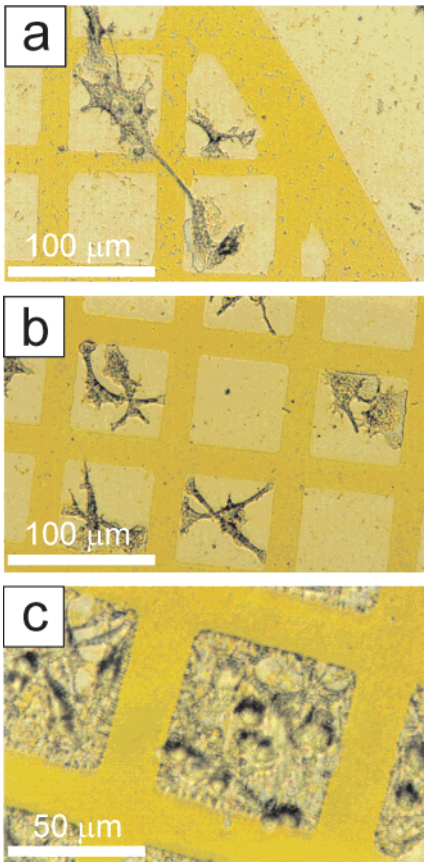

Figure 3. Optical micrographs of (a) macrophages grown in micropatterned corrals in the absence of PEG. The lighter areas correspond to C16SH and the darker areas to 3-PAA. (b) Macrophages grown at low density on a micropatterned film having a conformal layer of PEG grafted onto the 3-PAA walls. The light areas are C16SH and the darker areas are 3-PAA/PEG. (c) Same as (b), but the cells are present at higher density (note change in scale). Even at very high density, the cells are unable to cross the 3-PAA/PEG walls.

Part a of Figure 4 is a TM-AFM image of a macrophage cell confined within a single corral. The AFM micrograph clearly shows numerous filopodia emanating from the macrophages, but none that extends across the 3-PAA/PEG boundary. This image,

(59) López, G. P.; Biebuyck, H. A.; Harter, R.; Kumar, A.; Whitesides, G. M. *J. Am. Chem. Soc.* **1993**, *115*, 10774−10781.
(60) Lewandowska, K.; Pergament, E.; Sukenik, C. N.; Culp, L. A. *J. Biomed. Mater. Res.* **1992**, *26*, 1343−1363.
(61) In a previous study (Lackowski, W. M.; Franchina, J. G.; Bergbreiter, D. E.; Crooks, R. M. *Adv. Mater.* **1999**, *11*, 1368−1371), we showed that 3-PAA films had a rms roughness of 0.8 nm, and 2.0 nm for the C16SH-modified Au surfaces. Previous studies revealed that cell adhesion and migration increase with increasing surface roughness. (Lampin, M.; Warocquier-Clerout, R.; Legris, C.; Degrange, C.; Sigot-Luizard, M. F. *J. Biomed. Mater. Res.* **1997**, *36*, 99−108).
(62) Nuzzo, R. G.; Dubois, L. H.; Allara, D. L. *J. Am. Chem. Soc.* **1990**, *112*, 558−569.
(63) Bain, C. D.; Troughton, E. B.; Tao, Y. T.; Evall, J.; Whitesides, G. M.; Nuzzo, R. G. *J. Am. Chem. Soc.* **1989**, *111*, 321−335.
(64) Klein, C. L.; Scholl, M.; Maelicke, A. *J. Mater. Sci.: Mater. Med.* **1999**, *10*, 721−727.

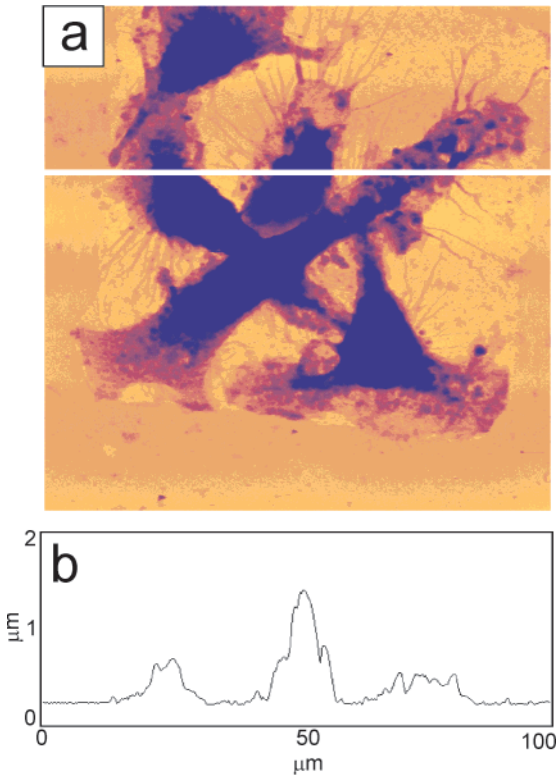

Figure 4. (a) 100 μm × 100 μm TM-AFM image of a macrophage growing in a corral. Note the filopodia, which are not visible in the optical micrographs, stop at the 3-PAA/PEG wall. (b) A line scan across the white line in (a). Note that the cell is more than 1 μm in height, while the 3-PAA/PEG pattern is only ~50 nm in height.

along with the line scan shown in part b, further demonstrates that cells are able to spread and grow within a given corral but that migration does not occur across the barriers because of the presence of the PEG graft. The line scan emphasizes that the cell is much higher (>1 μm) than the ~50-nm wall that confines it, which is not even apparent at the scale shown in this figure. Lamillipod extension can occur onto the 3-PAA/PEG boundary, as is apparent in the lower left of the image. However, the degree of extension is insufficient to cross the boundary.

As shown in Figure 5, endothelial cells and hepatocytes can also be grown on these three-dimensional patterned surfaces. Because of their large size, each corral generally contains only a single cell. We chose to study the adhesion and spreading of hepatocytes and endothelial cells due to their importance in the engineering of liver tissue. That is, spatial control and juxtaposition of these two cell types is necessary for correct liver function.[5,65] Although here we have patterned these cell types on different substrates, a straightforward extension of this methodology should allow us to co-culture them in vitro by protecting some of the corrals against cellular adhesion, culturing one cell type, deprotecting the protected corrals, and then co-culturing the second cell line.

The viability of cells confined within the corrals was investigated using a commercially available fluorescence live/dead assay that stains live cells green and dead cells red. Figure 6 shows a florescence micrograph of patterned macrophages stained using the live/dead viability assay (part a of Figure 6) and a corresponding bright-field image of the cells (part b). As evidenced by the green light emitted from the three corrals, the cells shown remained viable until the assay was performed regardless of whether a single cell was in the corral (center of image) or multiple cells were located in a single corral (corrals on the left and right of the image). Similar results were observed for patterned endothelial cells and hepatocytes. The fact that confined cells remain viable within the corrals is consistent with previous studies, which demonstrate that cells remain viable when patterned on relatively large areas (>~1000 μm^2) with apoptosis occurring in cells confined to smaller areas (<~1000 μm^2).[33−35] Our patterned corrals (~4000 μm^2) are large enough that the cells remain viable for up to three weeks.

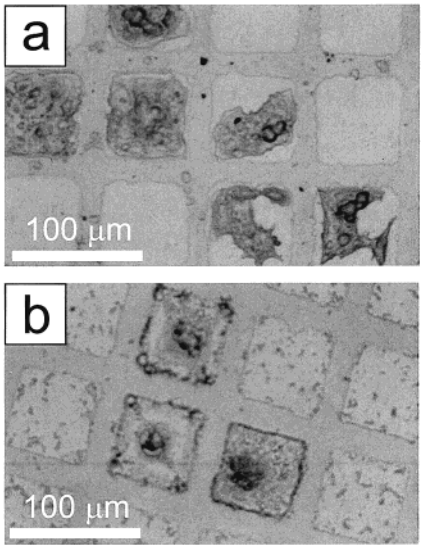

Figure 5. Optical micrographs of (a) endothelial cells and (b) hepatocytes confined within individual corrals.

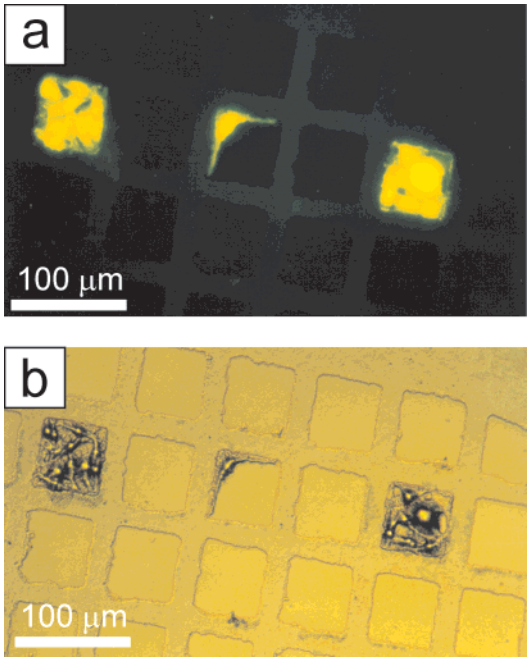

Figure 6. (a) Fluorescence micrograph of macrophages grown on a patterned substrate after performing a viability assay. The green color of the cells indicates that the cells were viable when the assay commenced. (b) Bright-field micrograph of the same area as in (a).

(65) Folch, A.; Toner, M. *Biotechnol. Prog.* **1998**, *14*, 388−392.

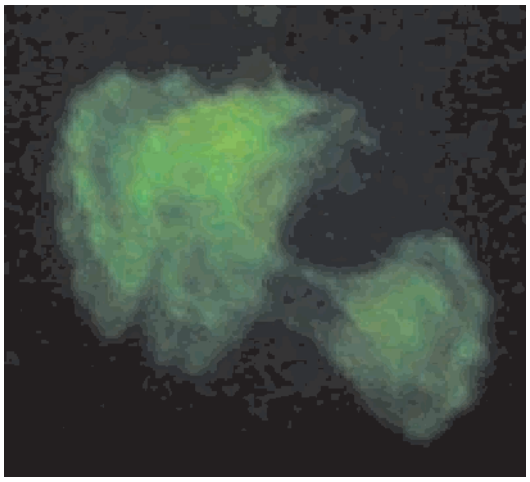

Figure 7. Fluorescence micrograph of the F-actin cytoskeleton of macrophages confined within corrals.

BODIPY-phallacidin was used to stain F-actin in micropatterned cells and investigate the effects of confinement on cell growth and spreading.[66] Figure 7 shows a fluorescence micrograph of the F-actin cytoskeleton of a small group of macrophages confined in a corral. The micrograph reveals that the actin skeleton is disorganized with the periphery of the cells apparently rich in actin. In the cell at the lower right, the actin distribution is polarized within the right edge of the cell suggesting the presence of a lamellipodium.[66]

CONCLUSIONS

Our studies demonstrate that growth of three different mammalian cell types (endothelial, hepatocytes, and macrophages) can be spatially directed on patterned surfaces consisting of cell corrals. These corrals are prepared using μCP-based lithography[45] of C16SH, which promotes cell adhesion and spreading within the corrals, followed by polymer grafting of 3-PAA/PEG, which prevents cellular adhesion.[54] The confined cells are viable and mobile within corrals, but neither cell bodies nor filopodia extend across the 3-PAA/PEG boundary. Although the polymeric patterns reported here are somewhat more time-consuming to prepare than those based exclusively on monolayers, we have found them to be more chemically versatile and less prone to defects and delamination.[51] One consequence of the three-dimensionality of the polymers is that they can be used to deliver small molecules and proteins to the nearby cells.[67]

We are presently using mammalian cells confined in high-density arrays like these as sensors for high-throughput screening. They may also find applications for tissue engineering, particularly if these methods can be translated to plastic substrates.[68]

ACKNOWLEDGMENT

We gratefully acknowledge the National Science Foundation (CHE-9818302), the Robert A. Welch Foundation, and the State of Texas Higher Education Coordinating Board through the Advanced Technology Program (010366-096 and 0082-1999) and the Advanced Research Program (036327-034). Support for this work was provided in part by the Interdisciplinary Research Initiatives Program, administered by the Office of the Vice President for Research and Associate Provost for Graduate Studies, Texas A&M University. In addition, R.M.C. acknowledges the U.S. Army Medical Research & Materiel Command and M.V.P. acknowledges support from the Alfred P. Sloan Foundation through a research fellowship.

Received for review August 3, 2000. Accepted January 17, 2001.

AC000907F

(66) Barber, K.; Mala, R. R.; Lambert, M. P.; Qui, R.; MacDonald, R. C.; Klein, W. L. *Neurosci. Lett.* **1996**, *207*, 17−20.

(67) Peez, R. F.; Dermody, D. L.; Franchina, J. G.; Jones, S. J.; Bruening, M. L.; Bergbreiter, D. E.; Crooks, R. M. *Langmuir* **1998**, *14*, 4232−4237.

(68) Ghosh, P.; Crooks, R. M. *J. Am. Chem. Soc.* **1999**, *121*, 8395−8396.